

THE OPTIMAL RATE FOR RESOLVING A NEAR-POLYTOMY IN A PHYLOGENY

MIKE STEEL AND CHRISTOPH LEUENBERGER

October 6, 2022

ABSTRACT. The reconstruction of phylogenetic trees from discrete character data typically relies on models that assume the characters evolve under a continuous-time Markov process operating at some overall rate λ . When λ is too high or too low, it becomes difficult to distinguish a short interior edge from a polytomy (the tree that results from collapsing the edge). In this note, we investigate the rate that maximizes the expected log-likelihood ratio (i.e. the Kullback–Leibler separation) between the four-leaf unresolved (star) tree and a four-leaf binary tree with interior edge length ϵ . For a simple two-state model, we show that as ϵ converges to 0 the optimal rate also converges to zero when the four pendant edges have equal length. However, when the four pendant branches have unequal length, two local optima can arise, and it is possible for the globally optimal rate to converge to a non-zero constant as $\epsilon \rightarrow 0$. Moreover, in the setting where the four pendant branches have equal lengths and either (i) we replace the two-state model by an infinite-state model or (ii) we retain the two-state model and replace the Kullback–Leibler separation by Euclidean distance as the maximization goal, then the optimal rate also converges to a non-zero constant.

1. INTRODUCTION

When discrete characters evolve on a phylogenetic tree under a continuous-time Markov process, the states at the leaves provide information about the identity of the underlying tree. It is known that when the overall substitution rates becomes too high or too low, it becomes increasingly impossible to distinguish the tree from a less resolved tree (or indeed from any other tree) using any given number of characters.

In particular, suppose we take a tree T with an interior edge e of length ϵ and we search for an overall substitution rate λ_ϵ that optimally discriminates (under some metric or criterion) between T_ϵ and T_0 (i.e. the tree that has the same topology and branch lengths as T_ϵ except that e has been collapsed (i.e. has length 0)). This optimal rate depends in an interesting way on the tree’s branch lengths (and the metric or criterion used), as revealed by several studies over the last two decades (see, for example, [2, 8, 10, 11, 13]), and applied to the study of data sets (see, for instance, [6, 12]).

In this short note, we consider a more delicate question that leads to some curious subtleties in its answer. Namely, how does λ_ϵ behave as ϵ tends to zero? For simplicity, we consider the four-leaf tree and two simple substitution models. We find that the answer to this question depends rather crucially on three things: whether the state space is finite or infinite, the metric employed, and the degree of imbalance in the branch lengths. Our results provide some analytic insight into simulation-based findings reported by [6] (in the second part of their section entitled ‘Optimum Rates of Evolution’);

Key words and phrases. Phylogenetic tree, Markov process, Optimal rate, Kullback–Leibler separation, Fisher information.

specifically, the optimal rate in the finite-state setting can behave differently from the optimal rate for generating characters that are parsimony-informative and homoplasy-free.

2. OPTIMAL RATE RESULTS

Consider a binary phylogenetic tree T_ϵ with four pendant edges of length L and an interior edge of length ϵ , as shown in Fig. 1(i). Now consider a Markovian process that generates states at the leaves of $T_\epsilon \geq 0$. We consider two models in this paper: (a) the two-state symmetric model (sometimes referred to as the Neyman two-state model or the Cavender-Farris-Neyman model), and (b) an infinite-allele model (in which a change of state always leads to a new state, a model often referred to as the infinite alleles model of Crow and Kimura [5], or the random cluster model [9]). For both models the induced partition of the leaf set (in which the blocks are the subsets of leaves in the same state) will be referred to as a *character*. Thus for the two-state model, there are exactly eight possible characters that can arise on T_ϵ , while for the infinite-allele model, there are 13 when $\epsilon > 0$ or 12 when $\epsilon = 0$ (there are 15 partitions of the set of four leaves of T_ϵ , however when $\epsilon > 0$ (resp. $\epsilon = 0$) two (resp. three) have zero probability of being generated).

Suppose that the branch lengths are all multiplied by a rate factor $\lambda \geq 0$, and let P_ϵ be the probability distribution on characters. Let P_0 be the probability distribution on characters under the corresponding model on the star tree T_0 (shown in Fig. 1(ii)).

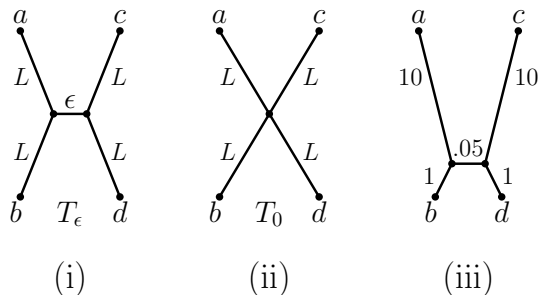


FIGURE 1. (i) A binary four-leaf tree T_ϵ with a short interior edge of length ϵ and four pendant edges of equal length L . (ii) The star tree obtained from T_ϵ by setting $\epsilon = 0$. (iii) A tree exhibiting two local optima for the rate λ maximizing $d_{\text{KL}}(P_0, P_\epsilon)$.

Now, suppose that a data set D of k characters is generated by an independent and identically distributed (i.i.d.) process on the (unresolved) star tree T_0 (under either Model (a) or Model (b)). Let LLR denote the log-likelihood ratio of the star tree T_0 to the resolved tree T_ϵ (i.e. the logarithm of the ratio $\mathbb{P}(D|T_0)/\mathbb{P}(D|T_\epsilon)$). As k grows, $\frac{1}{k}$ LLR converges in probability to its (constant) expected value, which is precisely the Kullback–Leibler separation (see [1]):

$$d_{\text{KL}}(P_0, P_\epsilon) = \sum_i P_0(i) \ln \left(\frac{P_0(i)}{P_\epsilon(i)} \right),$$

where the summation is over all the possible characters.

Let λ_ϵ be a value of λ that maximizes $d_{\text{KL}}(P_0, P_\epsilon)$. From the previous paragraph, this is the rate that provides the largest expected likelihood ratio in favour of the generating tree T_0 over an alternative resolved tree with an internal edge of length ϵ . We are interested in what happens to λ_ϵ as ϵ tends to zero. In that case, $d_{\text{KL}}(P_0, P_\epsilon)$ also converges to zero, but it is not immediately clear whether the optimal

rate that helps to distinguish T_0 from T_ϵ by maximizing $d_{\text{KL}}(P_0, P_\epsilon)$ should be increasing, decreasing or converging to some constant value. A large rate improves the probability of a state-change occurring on the central edge of T_ϵ however, this comes at the price of greater randomization on the pendant edges, which tends to obscure the signal of such a change based on just the states at the leaves.

It turns out that the limiting behaviour of λ_ϵ depends crucially on whether the state space is finite or infinite. In Part (i) of the following theorem, we consider just the two-state symmetric model (see e.g. Chapter 7 of [9]) but we indicate in Fig. 5 that a similar result appears to hold for the symmetric model on any number of states. The result in Part (i) contrasts with that in Part (ii) for the infinite-allele model, in which homoplasy (i.e. substitution to a state that has appeared elsewhere in the tree) does not arise. This second result is different from (but consistent with) a related result in [10].

Theorem 1.

(i) *For the two-state symmetric model,*

$$\lim_{\epsilon \rightarrow 0} \lambda_\epsilon = 0.$$

(ii) *By contrast, for the infinite-allele model,*

$$\lim_{\epsilon \rightarrow 0} \lambda_\epsilon = \frac{1}{4L}.$$

Proof. Part (i) Let $p = \frac{1}{2}(1 - \exp(-2\lambda\epsilon))$ be the probability of a state change across the interior edge of T_ϵ under the two-state model. Let p_1 be the probability of generating a character on T_ϵ , where one leaf is in one partition block and the other three leaves are in a different partition block, and let q_1 be the corresponding probability on T_0 . Because the four pendant edges of T_ϵ and T_0 have equal length, we have:

$$(1) \quad p_1 = (1 - p)q_1 + pq_1 = q_1,$$

so $q_1 \ln(q_1/p_1) = 0$.

Let p_2 be the probability of generating either one of the two characters that have a parsimony score of 2 on T_ϵ , and let q_2 be the corresponding probability on T_0 . Once again we have:

$$(2) \quad p_2 = (1 - p)q_2 + pq_2 = q_2,$$

and so $q_2 \ln(q_2/p_2) = 0$.

Let p_{12} be the probability of generating the character that has a parsimony score of 1 on T_ϵ and a parsimony score of 2 on T_0 , and let q_{12} be the corresponding probability on T_0 . Let p_0 be the probability of generating the character that has parsimony score 0 on T_ϵ and let q_0 be the corresponding probability on T_0 . Notice that we can write:

$$(3) \quad q_0 = \alpha^4 + (1 - \alpha)^4 \text{ and } q_{12} = 2\alpha^2(1 - \alpha)^2,$$

where $\alpha = \frac{1}{2}(1 - e^{-2\lambda L})$. Moreover,

$$p_{12} = (1 - p)q_{12} + pq_0,$$

and

$$p_0 = (1 - p)q_0 + pq_{12}.$$

It follows that

$$(4) \quad q_{12} \ln(q_{12}/p_{12}) = -q_{12} \ln(p_{12}/q_{12}) = -q_{12} \ln(1 - p + pq_0/q_{12})$$

and

$$(5) \quad q_0 \ln(q_0/p_0) = -q_0 \ln(p_0/q_0) = -q_0 \ln(1 - p + pq_{12}/q_0).$$

Combining Eqns. (1)–(5) gives:

$$d_{\text{KL}}(P_0, P_\epsilon) = 0 + 0 - q_{12} \ln \left(1 - p + \frac{q_0}{q_{12}} p \right) - q_0 \ln \left(1 - p + \frac{q_{12}}{q_0} p \right).$$

If we let $\theta = \theta(\lambda) = q_{12}/q_0$, then:

$$(6) \quad d_{\text{KL}}(P_0, P_\epsilon) = -q_0 \left(\theta \ln(1 + (1 - \theta) \frac{p}{\theta}) + \ln(1 - (1 - \theta)p) \right).$$

Notice that, by Eqn. (3), we have:

$$\theta = \frac{2\alpha^2(1 - \alpha)^2}{\alpha^4 + (1 - \alpha)^4} = \frac{2(1 - e^{-4\lambda L})^2}{(1 + e^{-2\lambda L})^4 + (1 - e^{-2\lambda L})^4},$$

and so, in Eqn. (6), θ is a monotone increasing function from 0 (at $\lambda = 0$) to a limiting value of 1 as $\lambda \rightarrow \infty$. Note also that $q_0 = q_0(\lambda)$ is a monotone decreasing function from 1 (at $\lambda = 0$) to a limiting value of $\frac{1}{8}$ as $\lambda \rightarrow \infty$.

Now let us set $\lambda = \lambda_x := x\epsilon$ in Eqn. (6), for a fixed value of x . Then

$$p = \frac{1}{2}(1 - \exp(-2\epsilon^2 x)) = x\epsilon^2 + O(\epsilon^3),$$

and from Eqn. (3) we have $\theta = 2x^2 L^2 \epsilon^2 + O(\epsilon^3)$. Therefore:

$$(7) \quad \ell(x) := \lim_{\epsilon \rightarrow 0} d_{\text{KL}}(P_0, P_\epsilon)/\epsilon^2 = -2x^2 L^2 \ln \left(1 + \frac{1}{2xL^2} \right) + x,$$

and so $\ell(x)$ converges to $\frac{1}{4L^2}$ as $x \rightarrow \infty$.

Next, suppose that λ_ϵ does not converge to zero as $\epsilon \rightarrow 0$. Then for some $\delta > 0$ and some sequence of values ϵ_i which converges to zero, we have:

$$(8) \quad \lambda_{\epsilon_i} > \delta > 0$$

for all i . Let $\lambda_i := \lambda_{\epsilon_i}$, $\theta_i := \theta(\lambda_i)$ and $p_i := \frac{1}{2}(1 - e^{-2\lambda_i \epsilon_i})$. Notice that $(1 - \theta_i)p_i$ converges to zero as $i \rightarrow \infty$. This is because we can write $0 \leq (1 - \theta_i)p_i \leq Ae^{-B\lambda_i}(1 - e^{-2\lambda_i \epsilon_i})$ for constants $A, B > 0$, and differential calculus shows that the maximal value of $Ae^{-B\lambda}(1 - e^{-2\lambda\epsilon})$ as $\lambda > 0$ varies converges to zero as $\epsilon \rightarrow 0$. Since θ_i is bounded away from 0 (by Inequality (8)), it also follows that $(1/\theta_i - 1)p_i = (1 - \theta_i)p_i/\theta_i$ converges to zero as $i \rightarrow \infty$.

Consequently, both $(1 - \theta_i)p$ and $(1 - \theta_i)p/\theta_i$ will both lie within $(0, 1)$ for all $i \geq I$ for some sufficiently large finite value I (dependent on δ). We now apply the following inequality and expansion which hold for all $x, y \in (0, 1)$:

$$-\ln(1 + x) < -x + \frac{x^2}{2}, \quad \text{and} \quad -\ln(1 - y) = \sum_{j \geq 1} \frac{y^j}{j}$$

with $x = (1 - \theta_i)p_i/\theta_i$ and $y = (1 - \theta_i)p_i$ in Eqn. (6). Noting that the two linear terms in p_i from Eqn. (6) cancel we obtain only quadratic and higher terms in p_i . Thus, for all $i \geq I$:

$$(9) \quad d_{\text{KL}}(P_0, P_\epsilon) < q_0(\lambda_i) \left[\frac{p_i^2}{2}(1 - \theta_i) \left(\frac{1}{\theta_i} - \theta_i \right) + \sum_{j \geq 3} \frac{(1 - \theta_i)^j p_i^j}{j} \right].$$

Moreover, $q_0(\lambda_i) < q_0(0) = 1$ (by Eqn. (8)) and $p_i \leq \lambda_i \epsilon_i$ for all i , so we can write:

$$(10) \quad \frac{d_{\text{KL}}(P_0, P_\epsilon)}{\epsilon_i^2} < \left[\frac{\lambda_i^2}{2} (1 - \theta_i) \left(\frac{1}{\theta_i} - \theta_i \right) \right] + \left[\frac{\epsilon_i}{2} \sum_{j \geq 3} \frac{(1 - \theta_i)^j \lambda_i^j \epsilon_i^{j-3}}{j} \right].$$

Let $y(t) = \frac{2(1-e^{-2t})^2}{(1+e^{-t})^4 + (1-e^{-t})^4}$. It can be verified that $\frac{t^2}{2}(1-y(t)) \left(\frac{1}{y(t)} - y(t) \right) < 1$ for all $t > 0$. Applying this with $t = 2\lambda_i L$, we obtain the following bound on the first term in Inequality (10):

$$\left[\frac{\lambda_i^2}{2} (1 - \theta_i) \left(\frac{1}{\theta_i} - \theta_i \right) \right] < \frac{1}{4L^2}.$$

In addition, the second term on the right in Inequality (10) converges to zero as i grows, since the summation term is absolutely bounded (note that $\lambda_i(1 - \theta_i) \rightarrow 0$ as $\lambda_i \rightarrow \infty$) and since the numerator term out front, ϵ_i , converges to 0.

In summary, for sufficiently large values of i , we have $d_{\text{KL}}(P_0, P_\epsilon)/\epsilon_i^2 < \frac{1}{4L^2}$. Thus, by selecting x sufficiently large we can ensure that $\ell(x)$ (given by Eqn. (7), and which is based on a λ value that converges to zero as $\epsilon \rightarrow 0$) takes a larger value for $d_{\text{KL}}(P_0, P_\epsilon)$ than the value λ_i . This completes the proof of Part (i).

For Part (ii), let $y = 1 - \exp(-\lambda L)$ and let $\zeta = 1 - \exp(-\lambda \epsilon)$; these are the probabilities of a state change on a pendant and the interior edge, respectively, in the infinite-allele model. For $i = 1, 2, 3, 4$, let $P_0[i]$ (resp. $P_\epsilon[i]$) be the probability of generating a partition on T_0 consisting of i blocks; with the restriction that for $i = 2$ the blocks must be of sizes (1, 3) (these are the only block sizes that T_0 can generate with strictly positive probability). We have:

$$P_0[1] = (1-y)^4, P_0[2] = 4y(1-y)^3, P_0[3] = 6y^2(1-y)^2, P_0[4] = 4y^3(1-y) + y^4.$$

Let $P_\epsilon[i]$ be the corresponding probabilities of T_ϵ . We can then write:

$$(11) \quad P_\epsilon[i] = (1 - \zeta)P_0[i] + \zeta D_i,$$

where D_i is dependent only on y . More precisely,

$$(12) \quad D_1 = D_2 = 0, D_3 = 2e^{-2\lambda L}(1 - e^{-2\lambda L}), D_4 = (1 - e^{-2\lambda L})^2.$$

The expression for D_3 arises because when there is a state change across the interior edge of T_ϵ then a partition of type (1, 1, 2) occurs precisely when there is no state change between the two leaves on one side of the edge (with probability $e^{-2\lambda L}$) and there is a state change between the two leaves on the other side of the edge (with probability $1 - e^{-2\lambda L}$); the coefficient out of 2 out front recognises that there are two ways that this can occur. For D_4 , a state change across the interior edge of T_ϵ leads to a partition of type (1, 1, 1, 1) precisely if the leaves on one side of the interior edge are in different states, and so too are the leaves on the other side of the interior edges, and these two independent events have probability $1 - e^{-2\lambda L}$. Thus,

$$(13) \quad d_{\text{KL}}(P_0, P_\epsilon) = - \sum_{i=1}^4 P_0[i] \ln(P_\epsilon[i]/P_0[i]) = - \sum_{i=1}^4 P_0[i] \ln \left(1 - \zeta \left(\frac{P_0[i] - D_i}{P_0[i]} \right) \right).$$

Substituting in the expressions for $P_0[i]$ and D_i above gives the following expression for $d_{\text{KL}}(P_0, P_\epsilon)$:

$$(14) \quad - [e^{-4\lambda L} + 4e^{-3\lambda L}(1 - e^{-\lambda L})] \ln(1 - \zeta) - 6e^{-2\lambda L}(1 - e^{-\lambda L})^2 \ln \left(1 - \zeta \left(1 - \frac{2e^{-2\lambda L}(1 - e^{-2\lambda L})}{6e^{-2\lambda L}(1 - e^{-\lambda L})^2} \right) \right) \\ - [4(1 - e^{-\lambda L})^3 e^{-\lambda L} + (1 - e^{-\lambda L})^4] \ln \left(1 - \zeta \left(1 - \frac{(1 - e^{-2\lambda L})^2}{4(1 - e^{-\lambda L})^3 e^{-\lambda L} + (1 - e^{-\lambda L})^4} \right) \right).$$

Now, T_ϵ has one additional partition type that it can generate but T_0 can not, namely the partition $\{\{a, b\}, \{c, d\}\}$. This partition is generated by T_ϵ with probability $\zeta e^{-4\lambda L}$ and so $\sum_{i=1}^4 P_\epsilon[i] = 1 - \zeta e^{-4\lambda L}$ (recall that $i = 2$ counts only partitions into blocks of sizes $(1, 3)$). By Eqn. (11), we obtain the identity

$$1 - \zeta e^{-4\lambda L} = \sum_{i=1}^4 P_\epsilon[i] = (1 - \zeta) \sum_{i=1}^4 P_0[i] + \zeta \sum_{i=1}^4 D_i = \sum_{i=1}^4 P_0[i] - \zeta \sum_{i=1}^4 (P_0[i] - D_i),$$

and since $\sum_{i=1}^4 P_0[i] = 1$ we deduce that:

$$(15) \quad \sum_{i=1}^4 (P_0[i] - D_i) = e^{-4\lambda L},$$

which is equivalent to the identity $D_1 + D_2 + D_3 + D_4 = 1 - e^{-4\lambda L}$ from Eqn. (12).

Now, $-\ln(1 - x) \geq x$ for all values of $x < 1$ and combining this with Eqns. (13) and (15) gives

$$(16) \quad d_{\text{KL}}(P_0, P_\epsilon) \geq \sum_{i=1}^4 P_0[i] \cdot \zeta \frac{(P_0[i] - D_i)}{P_0[i]} = \zeta \sum_{i=1}^4 (P_0[i] - D_i) = \zeta e^{-4\lambda L}.$$

By Eqn. (13) we can write $d_{\text{KL}}(P_0, P_\epsilon) = -\sum_{i=1}^4 a_i \ln(1 - \zeta b_i)$, where a_i and b_i are functions of λ defined by for $i = 1, 2, 3, 4$ by $a_i = P_0[i]$, $b_1 = b_2 = 1$ and

$$b_3 = \frac{a_3 - D_3}{a_3} = \frac{2(1 - 2e^{-\lambda L})}{3(1 - e^{-\lambda L})}, \quad b_4 = \frac{-4e^{-2\lambda L}}{(1 - e^{-\lambda L})(1 + 3e^{-\lambda L})}.$$

For $0 \leq \epsilon < L$ we have $|\zeta b_i| < 1$ for each value of i . This is clear for $i = 1, 2$; the cases $i = 3$ and $i = 4$ require a little care as $b_3, b_4 \rightarrow -\infty$ as $\lambda \rightarrow 0$. However, ζ also depends on λ and for $0 \leq \epsilon < L$ we have

$$|\zeta b_3| \leq \frac{2(1 - e^{-\lambda \epsilon})}{3(1 - e^{-\lambda L})} < \frac{2}{3} \quad \text{and} \quad |\zeta b_4| \leq \frac{1 - e^{-\lambda \epsilon}}{1 - e^{-\lambda L}} < 1.$$

Thus we expand Eqn. (13) via its Taylor series and write $d_{\text{KL}}(P_0, P_\epsilon) = \sum_{i=1}^4 a_i \sum_{j \geq 1} \frac{b_i^j \zeta^j}{j}$, and since the term for $j = 1$ is the term $\zeta e^{-4\lambda L}$ appearing in the lower bound for $d_{\text{KL}}(P_0, P_\epsilon)$ (see Eqn. ((16))), we have:

$$(17) \quad 0 \leq d_{\text{KL}}(P_0, P_\epsilon) - \zeta e^{-4\lambda L} \leq \sum_{i=1}^4 a_i \sum_{j \geq 2} \frac{|b_i|^j \zeta^j}{j}.$$

Notice that the term on the right of this last inequality can be written as $\zeta^2 \cdot \sum_{i=1}^4 a_i |b_i|^2 \cdot \sum_{j \geq 2} \frac{(|b_i| \zeta)^{j-2}}{j}$. For each $i = 1, 2, 3, 4$ the term $a_i |b_i|^2$ is bounded above by a constant times $e^{-\lambda L}$ (this is clear for $i = 1, 2$ and the above formulae for b_3, b_4 ensure it also holds for $i = 3, 4$ as there is a term $(1 - e^{-\lambda L})^2$ in a_i to cancel this term in the denominator of b_i^2). Consequently, from (17), we can write

$$(18) \quad 0 \leq d_{\text{KL}}(P_0, P_\epsilon) - \zeta e^{-4\lambda L} \leq \zeta^2 C e^{-c\lambda},$$

where C, c are absolute and strictly positive constants (not dependent on λ or ϵ).

By differential calculus, $\lambda'_\epsilon = \frac{1}{\epsilon} \ln\left(1 + \frac{\epsilon}{4L}\right)$ maximizes $\zeta e^{-4\lambda L}$, and $\lim_{\epsilon \rightarrow 0} \lambda'_\epsilon = \frac{1}{4L}$. Now for the value of λ_ϵ that maximizes $d_{\text{KL}}(P_0, P_\epsilon)$, Eqn. (18) shows that $\epsilon \lambda_\epsilon$ must tend to zero as $\epsilon \rightarrow 0$, since otherwise there is a sequence of values λ_{ϵ_i} which tends to infinity, which leads to values for $d_{\text{KL}}(P_0, P_\epsilon)$ that are smaller than those obtained by setting $\lambda = \lambda'_\epsilon$ (due to the exponential terms in Eqn. (18)) which contradicts the optimality assumption on λ_ϵ . Thus $\epsilon \lambda_\epsilon \rightarrow 0$ as $\epsilon \rightarrow 0$ which implies that $\lim_{\epsilon \rightarrow 0} d_{\text{KL}}(P_0, P_\epsilon)/\epsilon = \lambda e^{-4\lambda L}$, and this is maximized when $\lambda = \frac{1}{4L}$. This completes the proof of Part (ii). \square

Despite the contrast exhibited by Theorem 1 between the infinite-allele and two-state setting we have a curious correspondence between the models for the Euclidean metric (i.e. the L^2 metric), as the following result shows.

Theorem 2. *For the Euclidean metric d_2 , the substitution rate value λ that maximizes $d_2(P_0, P_\epsilon)$ is given by $\lambda = \frac{1}{2\epsilon} \ln(1 + \frac{\epsilon}{2L})$, which converges to $\frac{1}{4L}$ as $\epsilon \rightarrow 0$.*

Proof. Using the Hadamard representation for the two-state symmetric model [4], an associated inner product identity (Eqn. 7.28 in [9]) shows that:

$$(19) \quad d_2(P_0, P_\epsilon) = \frac{1}{\sqrt{2}} e^{-4L\lambda} (1 - e^{-2\lambda\epsilon}).$$

This function of λ has a unique local maximum at $\lambda = \frac{1}{2\epsilon} \ln(1 + \frac{\epsilon}{2L})$. Now, $\lim_{\epsilon \rightarrow 0} \frac{1}{2\epsilon} \ln(1 + \frac{\epsilon}{2L}) = \frac{1}{4L}$, and at this value of λ we have $\lim_{\epsilon \rightarrow 0} d_2(P_0, P_\epsilon)/\epsilon = \frac{1}{2\sqrt{2}} e^{-1}$. \square

Theorems 1 and 2 are illustrated in Fig. 2 and and Fig. 3. Here, the edge lengths of the tree are $L = 1$ (for each of the four pendant edges) and $\epsilon = 0.05$ and $\epsilon = 0.1$. The values were calculated using Eqns. (6) and (13) (using *Maple*), and are consistent with the expressions used in the derivation and statement of Theorems 1 and 2.

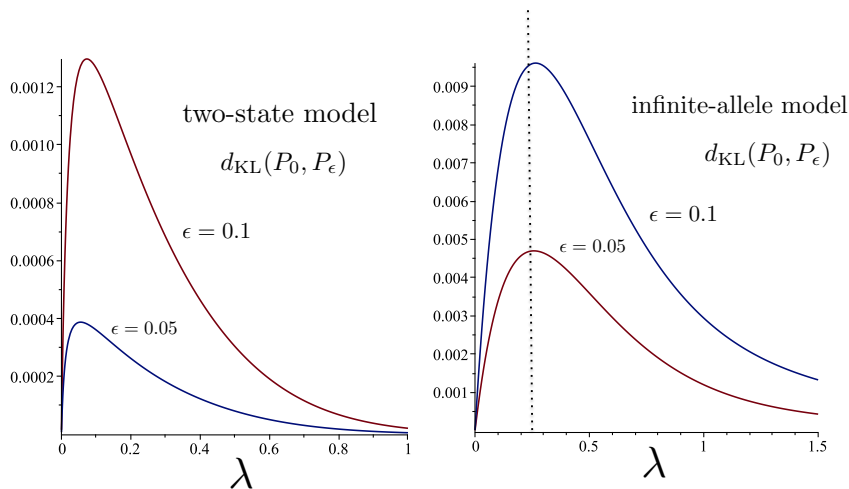


FIGURE 2. Kullback–Leibler separation of P_0 and P_ϵ for a quartet tree with exterior edges of lengths $L = 1$ and interior edge of length $\epsilon = 0.05$ and $\epsilon = 0.1$ as functions of λ , for the 2-state and infinite-allele models (calculated using Eqns. (6) and (13) respectively). The graph on the left is consistent with a progression of the optimal λ value towards zero as ϵ decreases, while for the infinite-allele model (right), the optimal λ value converges to $\frac{1}{4L} = 0.25$ as $\epsilon \rightarrow 0$, which gives the asymptotic value $\frac{\epsilon}{4L} e^{-1}$ for $d_{\text{KL}}(P_0, P_\epsilon)$.

The Kullback–Leibler separation is closely related to the Fisher information [7], and the usefulness of the Fisher information in phylogenetic trees has first been studied in [3]. It follows from large sample theory that the variance of an efficient estimator of the edge length ϵ , based on the data set D for a large number k of characters (and with L and λ being known), is inversely proportional to the Fisher

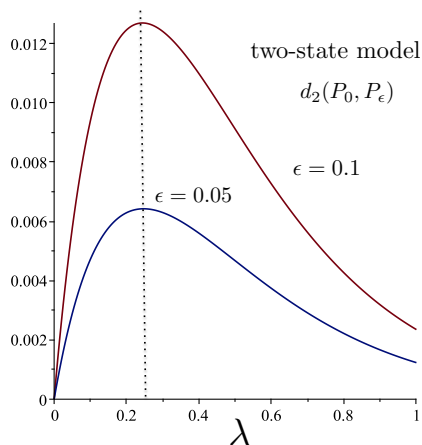


FIGURE 3. The Euclidean distance d_2 between P_0 and P_ϵ for a quartet tree with exterior edges of lengths $L = 1$ and interior edge of length $\epsilon = 0.05$ and $\epsilon = 0.1$ as functions of λ , for the 2-state model (calculated using Eqn. 19). The optimal λ value converges to $\frac{1}{4L} = 0.25$ as $\epsilon \rightarrow 0$, which gives the asymptotic value $\frac{\epsilon}{2\sqrt{2}}e^{-1}$ for $d_2(P_0, P_\epsilon)$.

information with respect to the parameter ϵ . The Fisher information is defined by:

$$I(\epsilon) = -\mathbb{E} \left[\frac{d^2}{d\epsilon^2} \ln P_\epsilon(i) \right] = -\sum_i P_\epsilon(i) \frac{d^2}{d\epsilon^2} \ln P_\epsilon(i).$$

Expanding $\ln P_\epsilon(i)$ in a Taylor series around $\epsilon = 0$, we get:

$$\begin{aligned} d_{\text{KL}}(P_0, P_\epsilon) &= \sum_i P_0(i) \ln \frac{P_0(i)}{P_\epsilon(i)} \\ &= \sum_i P_0(i) (\ln P_0(i) - \ln P_\epsilon(i)) \\ (20) \quad &= \sum_i P_0(i) \left(-\epsilon \frac{d}{d\epsilon} \Big|_{\epsilon=0} \ln P_\epsilon(i) - \frac{1}{2} \epsilon^2 \frac{d^2}{d\epsilon^2} \Big|_{\epsilon=0} \ln P_\epsilon(i) \right) + O(\epsilon^3) \\ &= -\epsilon \frac{d}{d\epsilon} \Big|_{\epsilon=0} \left(\sum_i P_\epsilon(i) \right) - \frac{1}{2} \epsilon^2 \sum_i P_0(i) \frac{d^2}{d\epsilon^2} \Big|_{\epsilon=0} \ln P_\epsilon(i) + O(\epsilon^3) \\ &= \frac{1}{2} \epsilon^2 I(0) + O(\epsilon^3). \end{aligned}$$

In the two-state model with $L = 1$, analysis of the coefficient of ϵ^2 in Eqn. (6) (using *Mathematica*) provides the following explicit description of the Fisher information term $I(0)$:

$$(21) \quad I(0) = \frac{8\lambda^2 \exp(-4\lambda) \cosh^2(2\lambda)}{(3 + \cosh(4\lambda)) \sinh^2(2\lambda)}.$$

Let $\hat{\epsilon}$ be an asymptotically efficient estimator of the short edge length, i.e. one whose variance asymptotically achieves the Cramér-Rao bound (see Ch. 6.2 in [7]). Then its relative error, based on a large number k of i.i.d. generated characters, is roughly

$$\text{relative error}(\hat{\epsilon}) := \frac{\sqrt{\text{var}(\hat{\epsilon})}}{\epsilon} \approx \frac{\sqrt{1/kI(\epsilon)}}{\epsilon}.$$

From (20), we get, for small values of ϵ , the approximation:

$$\text{relative error}(\hat{\epsilon}) \approx [2k d_{\text{KL}}(P_0, P_\epsilon)]^{-1}.$$

From this we see that the optimal rate λ_ϵ minimizes the relative estimation error for the edge length, again underlying the usefulness of Kullback–Leibler separation in our situation.

3. UNEQUAL PENDANT EDGE LENGTHS

Theorem 1(i) is not generally valid for quartets when we drop the assumption of equal edge lengths. Fig. 4 shows the Kullback–Leibler separation $d_{\text{KL}}(P_0, P_\epsilon)$ dependent on λ for a quartet tree with interior edge length $\epsilon = 0.05$ and unequal lengths of 1 and 10 on the pendant edges on one side of the interior edge e , and also 1 and 10 on the pendant edges on other side of e (as shown in Fig. 1(iii)).

There is still a local maximum which tends to 0 as $\epsilon \rightarrow 0$ but the global maximum λ_ϵ stays bounded away from 0.

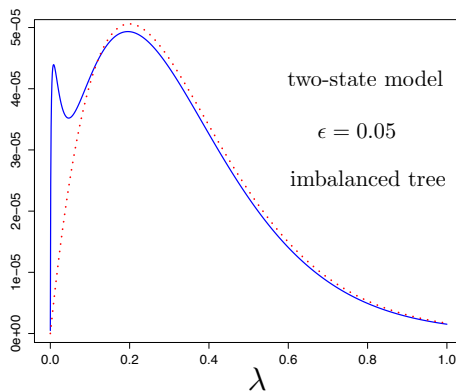


FIGURE 4. Kullback–Leibler separation (solid line) for a quartet tree with exterior edges of lengths 1 and 10 on both sides of the interior edge of length $\epsilon = 0.05$ as a function of λ . The dotted line shows the Fisher information term from Eqn. (22).

This idiosyncratic shape of the curve in the highly asymmetric case can be explained as follows: If two edges on each side of the central edge are very long, they can essentially be ignored (the state at each of the two leaves is almost completely random) and the states at the leaves of the two shorter edges of lengths 1 are more informative for inferring the total length of $2 + \epsilon$ of the path joining them, and thereby for deciding whether or not $\epsilon = 0$. Let

$$p(\epsilon) = \frac{1}{2} (1 + \exp(-2\lambda(2 + \epsilon)))$$

be the probability that the two characters at the leaves of the unit-length edges are in the same state. Then the Fisher information with respect to ϵ , when we ignore the characters at the leaves of the two long edges, is the given by:

$$\begin{aligned} (22) \quad I_2(\epsilon) &= -p(\epsilon) \frac{d^2}{d\epsilon^2} \ln p(\epsilon) - (1 - p(\epsilon)) \frac{d^2}{d\epsilon^2} \ln(1 - p(\epsilon)) \\ &= \frac{4\lambda^2}{\exp(4\lambda(2 + \epsilon)) - 1}. \end{aligned}$$

Fig. 4 shows $\epsilon^2 I_2(0)/2$ as a function of λ (the dotted line). Clearly, the global maximum is explained by the estimation of ϵ via the two unit-length edges. As for Fig. 2, the values were calculated by simulating characters over a range of λ values (using the R statistical package).

By lessening the imbalance between the pendant edge lengths it is possible to make the two local optima for the rates have equal (global) optimal values; which provides an example where the global optimal rate for maximizing $d_{\text{KL}}(P_0, P_\epsilon)$ is not unique. When the edge length imbalance decreases further, simulations suggest that Theorem 1(i) remains valid (i.e. the limit $\lambda_\epsilon \rightarrow 0$ as $\epsilon \rightarrow 0$ does not just hold for the special setting in which all pendant edges have exactly equal lengths).

3.1. Concluding comments. For the biologist, Theorem 1 (i) provides a caution: in resolving a near-polytomy, it is tempting to search for genetic data that have evolved fast enough to have undergone substitution events on the interior edge; however, a slower-evolving data set may, in fact, be more likely to distinguish the resolved tree from an unresolved phylogeny. For infinite-allele models, however, Theorem 1(ii) ensures there is a positive optimal rate regardless of how short the interior edge is (consistent with a related result from [10]). Theorem 1 applies to balanced trees, and we also saw that for sufficiently unbalanced trees, these findings can change due to the appearance of a second local optimal rate that eventually becomes the global optimal rate (*cf* Fig. 4). Moreover, as Fig 5 indicates, the results established for the two-state symmetric model appear to hold for other finite-state models such as the four-state symmetric model (often referred to as the ‘Jukes-Cantor (1969)’ model (JC69); for details see [9], Section 7.2.2).

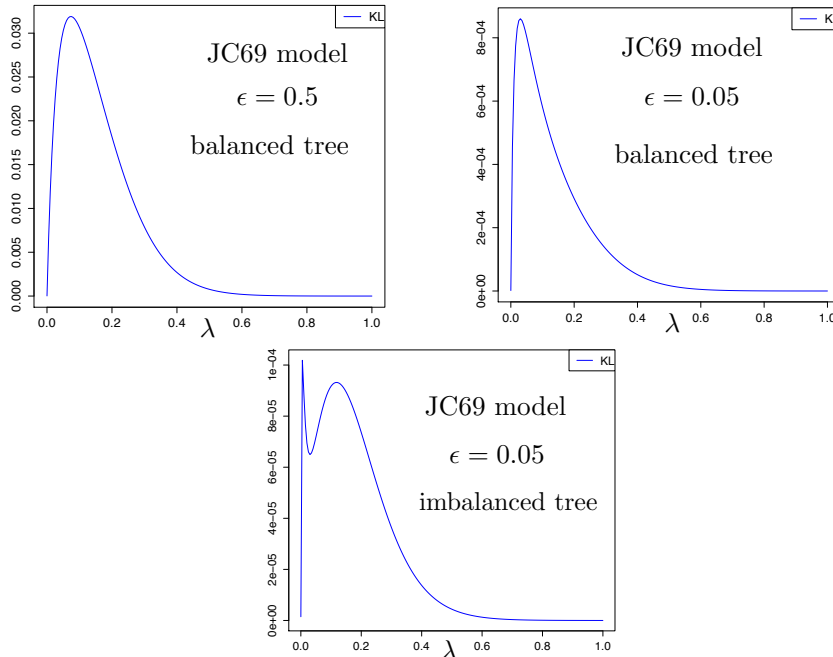


FIGURE 5. The four-state symmetric model (JC69) shows similar behaviour to the 2-state symmetric model. Top: Kullback–Leibler separation of P_0 and P_ϵ for a quartet tree with exterior edges of lengths $L = 1$ and interior edge of length $\epsilon = 0.5$ and $\epsilon = 0.05$ as functions of λ . Bottom: Kullback–Leibler separation of P_0 and P_ϵ for a quartet tree with exterior edges of lengths $L = 1$ and $L = 10$ as shown in Fig. 1(iii), and $\epsilon = 0.05$.

We have assumed throughout that the lengths of the four pendant edges of the tree remain fixed as the interior edge shrinks to zero. If the pendent edges are also allowed to shrink, then Theorem 1 no longer applies. For example, consider the binary tree T'_ϵ that has an interior edge of length ϵ and four pendant edges of length $L\epsilon$. Then as $\epsilon \rightarrow 0$, the optimal rate λ_ϵ now *increases* towards infinity rather than decreasing to zero as $\epsilon \rightarrow 0$. The reason for this is quite simple. Consider the tree T_1 that has an interior edges of length 1 and four pendant edges each of length L . This tree has some optimal rate λ^* that maximizes d_{KL} . Now T'_ϵ is obtained from T_1 by multiplying each edge length of T_1 by $\lambda\epsilon$. Thus, for T_ϵ , the optimal rate is given by $\lambda_\epsilon = \lambda^*/\epsilon \rightarrow \infty$ as $\epsilon \rightarrow 0$.

Finally, we have considered $d_{\text{KL}}(P_0, P_\epsilon)$ rather than $d_{\text{KL}}(P_\epsilon, P_0)$, partly because the former is easier to analyse mathematically, and is well-defined in the infinite-allele setting ($d_{\text{KL}}(P_\epsilon, P_0)$ is not well-defined for this model since the partition $\{\{a, b\}, \{c, d\}\}$ has positive probability under P_ϵ for $\epsilon > 0$ and zero probability under P_0). However, a more fundamental reason for our choice of $d_{\text{KL}}(P_0, P_\epsilon)$ is that it is more natural to consider the unresolved tree ($\epsilon = 0$) as the null hypothesis and the resolved tree as the alternative hypothesis because one typically wishes to disprove the null which in our case means to reject the polytomy.

4. ACKNOWLEDGEMENTS

We thank Jeffrey Townsend and Daniel Wegmann for helpful discussions. We also thank the three anonymous reviewers for numerous helpful suggestions that have improved the paper.

REFERENCES

- [1] Cover, T. M. and Thomas, J. A. (2006). Elements of Information Theory (2nd ed.) Wiley-Interscience.
- [2] Fischer, M. and Steel, M. (2009). Sequence length bounds for resolving a deep phylogenetic divergence. *J. Theor. Biol.* 256: 247–252.
- [3] Goldman, N. (1998). Phylogenetic information and experimental design in molecular systematics, *Proc. Roy. Soc. B* 265: 1779–1786.
- [4] Hendy, M. D. (1989). The relationship between simple evolutionary tree models and observable sequence data, *Syst. Biol.* 38: 310–321.
- [5] Kimura, M. and Crow, J (1964). The number of alleles that can be maintained in a finite population. *Genetics.* 49: 725–738.
- [6] Klopstein, S., Kropf, C. and Quicke, D.L.J. (2010). An evaluation of phylogenetic informativeness profiles and the molecular phylogeny of Diplazontinae (Hymenoptera, Ichneumonidae), *Syst. Biol.* 59(2): 226–241.
- [7] Lehmann, E. L. and Casella, G. (1998). Theory of point estimation (2nd ed.) Springer.
- [8] Lewis, P. O., Chen, M.-H., Luo, L., Lewis, L. A., Fučíková, K., Neupane, S., Wang, Y.-B. and Shi, D. (2016). Estimating Bayesian phylogenetic information content. *Syst. Biol.* 65(6): 1009–1023.
- [9] Steel, M. (2016). Phylogeny: discrete and random processes in evolution. CMBS-NSF Regional Conference Series in Applied Mathematics No. 89. SIAM Philadelphia PA.
- [10] Townsend, J.P. (2007). Profiling phylogenetic informativeness, *Syst. Biol.* 56(2): 222–231.
- [11] Townsend, J.P. and Leuenberger, C. (2011). Taxon sampling and the optimal rates of evolution for phylogenetic inference. *Syst Biol.* 60(3): 358–365.
- [12] Townsend J.P., Su Z, Tekle Y.L. (2012), Phylogenetic signal and noise: predicting the power of a data set to resolve phylogeny. *Syst. Biol.* 61(5): 835–849.
- [13] Yang, Z. (1998), On the best evolutionary rate for phylogenetic analysis. *Syst. Biol.* 47:125–133.

MS: BIOMATHEMATICS RESEARCH CENTRE, UNIVERSITY OF CANTERBURY, CHRISTCHURCH, NEW ZEALAND, CL: DÉPARTEMENT DE MATHÉMATIQUES, UNIVERSITÉ DE FRIBOURG, CHEMIN DU MUSÉE 3, 1705 FRIBOURG, SWITZERLAND

E-mail address: `mike.steel@canterbury.ac.nz`, `christoph.leuenberger@unifr.ch`